Bull. Mater. Sci., Vol. 34, No. 7, December 2011, pp. 1569–1573. © Indian Academy of Sciences.

Effect of ZnO loading technique on textural characteristic and methyl blue removal capacity of exfoliated graphite/ZnO composites

XUEQING YUE[†,††], WENYAN DUAN[††], YAN LU[††], FUCHENG ZHANG[††] and RUIJUN ZHANG[†,††,*]

[†]State Key Laboratory of Metastable Materials Science and Technology, Yanshan University, Qinhuangdao 066004, P.R. China

[††]Qinhuangdao Vocational and Technical College, Qinhuangdao 066100, P.R. China

MS received 28 September 2009; revised 17 February 2011

Abstract. Two exfoliated graphite/ZnO composites, marked as EG/ZnO-1 and EG/ZnO-2, were prepared by heating a mixture of expandable graphite and $Zn(OH)_2$ or a mixture of expanded graphite (EG) and $Zn(OH)_2$, respectively. The composites were characterized by scanning electron microscopy (SEM), X-ray diffraction (XRD) and nitrogen adsorption. Under UV irradiation, the composites were used for removing methyl blue (MB) from aqueous solution. For the composites made from expandable graphite (EG/ZnO-1), the micron-sized ZnO particle agglomerates (1–20 μm) heterogeneously distributed at the surface of graphite flakes, while for the composites made from EG (EG/ZnO-2), the submicron-sized ZnO particle masses (0·2–0·5 μm) almost homogeneously located both at the surface and interior of graphite flakes. In the presence of UV irradiation, the composites had the adsorption capacity of EG and the photocatalysis capacity of ZnO at the same time. Compared with EG/ZnO-1, EG/ZnO-2 was more effective in removing MB. After 2 h of UV irradiation, MB could be completely removed by using the EG/ZnO-2 containing 45% ZnO, and the decomposition efficiency of the ZnO was the primary cause for the removal of MB.

Keywords. Exfoliated graphite/ZnO; adsorption; decomposition; methyl blue.

1. Introduction

Wastewater containing various dyes is one of the major industrial pollutants. The photocatalytic decomposition of organic pollutants in wastewater received considerable research attention. Among the photocatalysts studied for their photocatalytic properties, TiO_2 is the most commonly used photocatalyst for its high efficiency, low cost, non-toxicity and photochemical stability. Recently, another photocatalyst, ZnO, is receiving great attention from researchers (Yeber *et al* 1999; Lizama *et al* 2002; Quintana *et al* 2002; Daneshvar *et al* 2003, Wang *et al* 2008). It was proved that ZnO displayed a similar photo-degradation mechanism as TiO_2 and therefore was proposed as a suitable alternative to TiO_2.

Exfoliated graphite (EG) is an excellent inorganic carbon material with a porous structure, which has many characteristics including low density, non-toxicity, non-pollution and easy disposal. Because of its porous structure, this material has been used as an absorbent for removing organic pollutants from wastewater, such as oils, biomedical liquids and dyes (Chung 1987; Toyoda and Inagaki 2000; Kang *et al* 2003; Tryba *et al* 2003, Zheng *et al* 2004; Li *et al* 2007). Moreover, EG is an excellent support for loading photocatalysts (Savoskin *et al* 2006; Shornikova *et al* 2008; Yue *et al* 2008).

EG/ZnO composites used in the discussion of this paper were prepared by using two different ZnO-loading methods. We attempted to investigate the effect of ZnO-loading methods on the texture characteristics and methyl blue (MB) removal capacities of the composites.

2. Experimental

2.1 *Materials*

Natural flake graphite (35 mesh, 99% purity, possible contaminants including silica, thorium and iron) was purchased from Qingdao Tianhe Graphite Company, China. Zn $(NO_3)_2{\cdot}6H_2O$, sulphuric acid (98%), hydrogen peroxide (30%), $CO(NH_2)_2$, ethanol and distilled water were of laboratory reagent grade and used without further purification.

2.2 *Preparation of the composites*

Natural flake graphite (6 g) was mixed with sulphuric acid as the intercalation agent (10 ml) and hydrogen peroxide as the oxidizing agent (1·0 ml). The mixture was left to stand at 50°C for 90 min, washed to pH 5–7 and

*Author for correspondence (yuexueqing@126.com)

dried at 70°C for 24 h, forming expandable graphite. EG could be obtained by abruptly heating the expandable graphite at 700°C for 40 s. The reaction equations for the preparation of ZnO could be described as follows:

$$CO(NH_2)_2 + 3H_2O \xrightarrow{\Delta} CO_2\uparrow + 2NH_3 \cdot H_2O, \quad (1)$$

$$Zn^{2+} + NH_3{\cdot}H_2O \rightarrow Zn(OH)_2\downarrow + 2NH_4^+, \quad (2)$$

$$Zn(OH)_2 \xrightarrow{\Delta} ZnO + H_2O\uparrow. \quad (3)$$

According to the (1) and (2), $Zn(OH)_2$ was prepared as follows: in a 1000 ml conical flask, $Zn(NO_3)_2{\cdot}6H_2O$ (0·1 mol/l) and $CO(NH_2)_2$ (0·3 mol/l) were dissolved in 500 ml distilled water under vigorous stirring at room temperature, dispersed by ultrasonication for 10 min, which resulted in a transparent solution. The transparent solution was stirred at 90°C for 3 h, forming a milk-like liquid. After stirring, the milk-like liquid was cooled to the room temperature, which resulted in the formation of white precipitate at the bottom of the conical flask. To get $Zn(OH)_2$, the white precipitate was collected by centrifugation and washed successively by distilled water and ethanol. According to the (3), ZnO could be obtained by heating the $Zn(OH)_2$ at 400°C for 3 h. A tunnelling electron microscopy (TEM) examination showed that the ZnO as-prepared was in the form of spherical particles with size of 40–60 nm and X-ray diffraction (XRD) measurement revealed that the structure resembled hexagonal wurtzite ZnO (the corresponding figures were not present here).

EG/ZnO-1 was prepared as follows: expandable graphite was mixed with $Zn(OH)_2$ solution, placed at 30–40°C for 3 days and dried at 70°C for 24 h, and finally heated at 700°C for 40 s and 400°C for 3 h. EG/ZnO-2 was prepared as follows: EG was mixed with $Zn(OH)_2$ solution, placed at 30–40°C for 3 days and dried at 70°C for 24 h, and finally heated at 400°C for 3 h. By changing the concentration of $Zn(NO_3)_2{\cdot}6H_2O$, the ZnO content in the composites ($W_{ZnO,}$ wt%) was controlled, which was measured by the complex titration analysis method. It was found that the permissible ZnO contents for EG/ZnO-1 and EG/ZnO-2 were about 35 and 85%, respectively.

2.3 *Characterization of the composites*

The phase composition of the composites was determined by X-ray diffraction (D/max-rB, Rigaku, Japan) (CuKα, 40 kV, 40 mA, 10–80°, 0·02 step, 10 s step^{-1}). Scanning electron microscopy (SEM, KY2828 type) was used to observe the morphology. Specific surface areas (S_{BET}) were measured by physical nitrogen adsorption measurement at 77 K.

2.4 *Removal of MB by the composites*

At room temperature, a 200 ml beaker was charged with MB aqueous solution (150 ml) at a concentration of 10 mg/l and the composites (0·15 g). The solution (pH = 7) was irradiated by a 30 W mercury lamp (UV-C, Philips) for 3 h. The UV lamp was positioned parallel to the solution, and the distance between the top of the solution and the UV lamp was constant (15 cm). UV-2501PC (Shimadzu, Japan) UV-Vis spectrometer (at λ_{max} 665 nm) was used to observe the removal of MB. For comparison, this solution was also placed for 3 h in the absence of UV irradiation. In the absence (or presence) of UV irradiation, the adsorption efficiency (or removal efficiency) was calculated by using the following equation:

$$\text{Adsorption efficiency (or removal efficiency)} = (A_{665,i} - A_{665,t})/A_{665,t}, \quad (4)$$

where $A_{665,i}$ is the absorbance of initial MB solution at 665 nm; $A_{665,t}$ is the absorbance (665 nm) at measurable time t.

Decomposition efficiency of the composites could be approximately denoted as

$$\text{Decomposition efficiency} = \text{removal efficiency} - \text{adsorption efficiency}. \quad (5)$$

3. Results and discussion

3.1 *SEM of the composites*

Representative SEM micrographs (figure 1) show the surface and interior structures of the composites. For EG/ZnO-1, the micron-sized ZnO particle agglomerates (1–20 μm) heterogeneously located at the surface of graphite flakes, as shown in figure 1(a, b). For EG/ZnO-2, however, the submicron-sized ZnO particle masses (0.2–0.5 μm) almost homogeneously located both at the surface and interior of graphite flakes, as shown in figure 1(c, d). The inner pores between the flakes were partly filled by ZnO particles, which decreased the total amount of the open pores. These observations could be explained by the difference between the preparation processes of the two composites. When expandable graphite was impregnated by $Zn(OH)_2$ solution, most of $Zn(OH)_2$ would locate at the surface of graphite flakes because most of graphite layers were closed (Yue *et al* 2008), and consequently most of the ZnO particles in EG/ZnO-1 located at the surface of graphite flakes. A study (Inagaki *et al* 2003) showed that most of the pores in EG were opened, and the porosity of the closed pores was less than 1%. As a consequence, $Zn(OH)_2$ could easily enter into the interior of graphite flakes when EG was mixed with $Zn(OH)_2$ solution. The difference between the permissible ZnO contents of the two composites is attributed to the reasons discussed above.

Table 1 shows the pore texture parameters and the removal efficiencies of the composites (average of three measurements). Compared with EG/ZnO-1, EG/ZnO-2

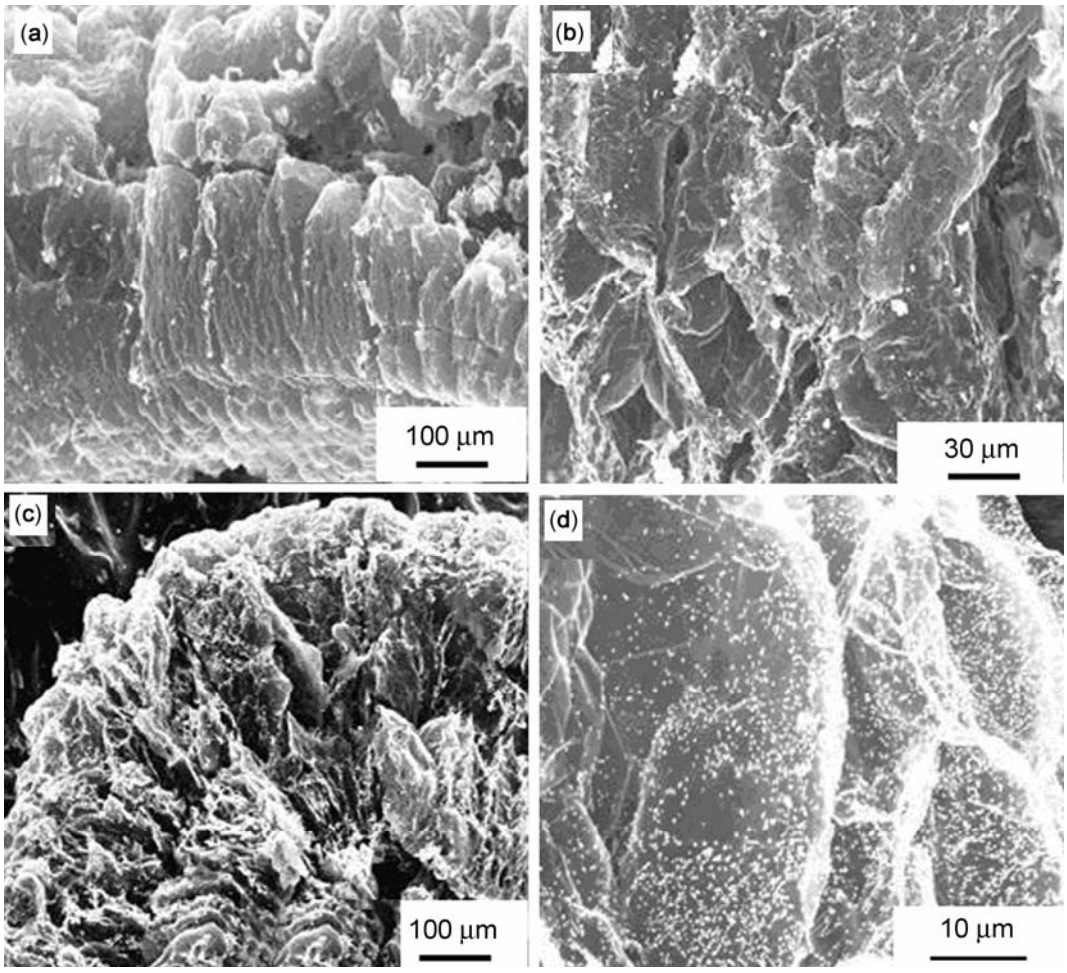

Figure 1. SEM micrographs showing surface and interior structures of composites.

Table 1. Pore texture parameters and MB removal capacities of the composites.

Sample	W_{ZnO} (wt%)	Exfoliation volume (ml/g)	S_{BET} (m^2/g)	Adsorption efficiency (3 h; %)	Removal efficiency (3 h; %)
Pure EG	0	250	50	31·4	33·0
EG/ZnO-1	25	160	44	26·0	70
EG/ZnO-1	35	150	43	25·1	75
EG/ZnO-2	25	35	15	25·2	74·9
EG/ZnO-2	35	30	13	22·4	83·6
EG/ZnO-2	45	30	13	20·0	100
EG/ZnO-2	55	25	12	18·3	89·0
EG/ZnO-2	65	20	10	18·0	73·9

exhibited far lower expanded volumes and specific surface areas, which could be explained by its dispersed EG particles (based on experimental observation), retracted surface V-type pores (figure 1c) and partly filled inner pores (figure 1d).

3.2 *XRD of the composites*

The XRD patterns of the composites are shown in figure 2. Besides the graphite (002) peaks, all the marked peaks could coincidently be indexed as the hexagonal wurtzite-type ZnO. Compared with EG/ZnO-2, EG/ZnO-1 exhibited less and weaker ZnO diffraction peaks, which might be due to its higher expanded volume (table 1) and larger ZnO particle agglomeration (figures 1a, b). In EG/ZnO-2, the relative high intensity of the ZnO (101) peak indicated anisotropic growth and presented a preferred orientation of the crystallites, but which was not the case for EG/ZnO-1. The reason needed further study.

3.3 *Removal of MB by the composites*

The composites only had the adsorption capacity of EG in the absence of UV irradiation, which was influenced by the EG content and the pore texture parameters of the composites. In the presence of UV irradiation, the composites had the adsorption capacity of EG and the photocatalysis capacity of ZnO at the same time. Table 1 showed that the difference between the adsorption efficiency and removal efficiency of the pure EG was negligible, but which was not the case for the composites. This suggested that the ZnO was necessary for the decomposition of MB, and the decomposition efficiency could be approximately denoted by the difference of removal efficiency and adsorption efficiency, as shown in (5). For EG/ZnO-1, the removal efficiency increased from 70 to 75% with increasing the ZnO content from 25 to 35% of the maximum content. For the same ZnO content of 35%, EG/ZnO-2 exhibited higher removal efficiency than EG/ZnO-1 did, which might be due to its more fine and uniform distribution of ZnO particles. For EG/ZnO-2, the removal efficiency increased with increasing the ZnO content up to 45% and then decreased, which could be explained by the two opposing effects with increasing the ZnO content. Increasing the ZnO content could strengthen the photocatalytic capacity of the composites, but weaken the adsorption capacity. Moreover, the bulk density of the composites would increase with increasing the ZnO content, causing the increase in the amount of the composites sink to bottom. Therefore, the optimal ZnO content in EG/ZnO-2 was 45%.

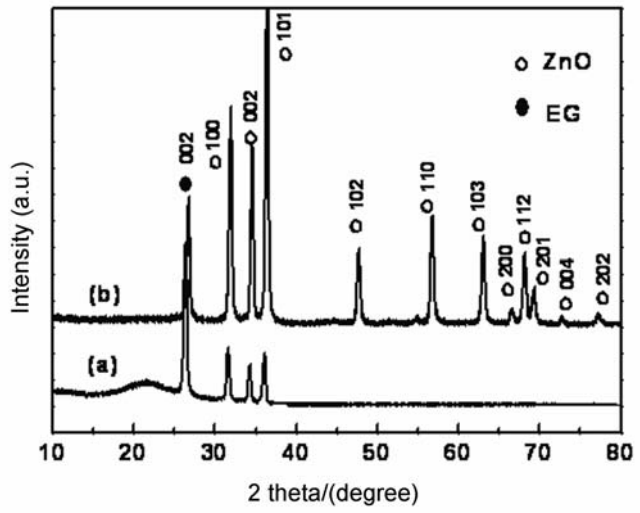

Figure 2. XRD patterns of composites.

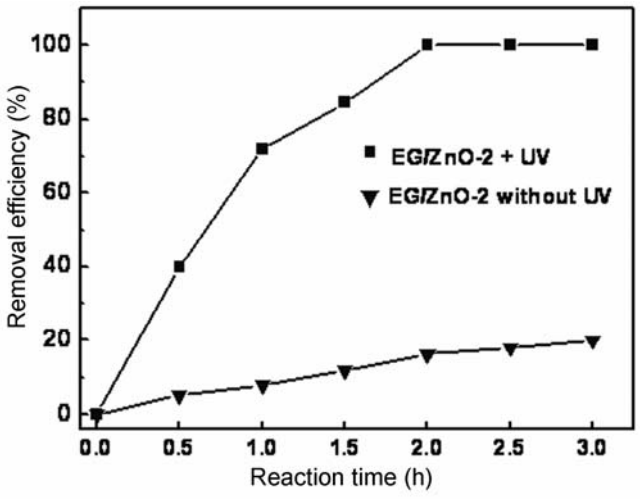

Figure 3. Effect of reaction time on adsorption and removal efficiency of EG/ZnO-2 with 45% ZnO.

Figure 3 shows the effect of reaction time on the adsorption and removal efficiency of the EG/ZnO-2 with 45% ZnO. The removal efficiency reached to 100% after 2 h UV irradiation, but the adsorption efficiency was only 20% at 3 h. This result indicated that, for the EG/ZnO-2, the decomposition efficiency of ZnO was the primary cause of the MB removal, while the main function of EG was to make the MB absorbed onto the composites and provide decomposition site. Due to the characteristic pore structure of EG, a large amount of UV could permeate through the pores and irradiate onto the ZnO particles on EG. Therefore, the removal system could provide a three-dimensional decomposition environment for the absorbed MB, which was not the case for the current supports, such as silica gel, glass, ceramic membrane and stainless steel. Loading photocatalyst on EG could combine the adsorption capacity of EG and the photocatalytic capacity of the photocatalyst, and effectively remove dye in water (Li *et al* 2008). However, this work did not deal with the effect of photocatalyst-loading technique on the removal capacity of EG/photocatalyst composites. In this paper, we used two different techniques to load photocatalyst on EG and found that photocatalyst-loading method strongly influenced the textural characteristic and dye removal capacity of EG/photocatalyst composites.

4. Conclusions

By using two ZnO-loading methods, we successfully synthesized two EG/ZnO composites. Compared with EG/ZnO-1, the distribution of ZnO particles in EG/ZnO-2 was more fine and uniform, and the permissible ZnO content in EG/ZnO-2 was larger. Under UV irradiation, the composites had the adsorption capacity of EG and the photocatalysis capacity of ZnO at the same time. EG/ZnO-2 was more effective and useful on removing MB compared with EG/ZnO-1. After 2 h UV irradiation, the removal efficiency could reach 100% by using the EG/ZnO-2 containing 45% ZnO, and the decomposition efficiency of the ZnO was the primary cause of MB removal.

Acknowledgements

This work was supported by the National Science Foundation for Distinguished Young Scholars of China (No. 50925522) and the National Science Foundation of China (No. 50975247).

References

Chung D D L 1987 *J. Mater. Sci.* **22** 4190

Daneshvar N, Rasoulifard M H, Khataee A R and Hosseinzadeh F 2007 *J. Hazard. Mater.* **143** 95

Inagaki M, Toyoda M, Kang F Y, Zhang Y P and Shen W C 2003 *New Carbon Mater.* **18** 241

Kang F Y, Zhang Y P, Zhao H N, Wang L N, Shen W C and Inagaki M 2003 *New Carbon Mater.* **18** 161

Li J H, Li M, Li J, Xu Y, Jia Z X and Li M 2008 *Ultrason. Sonochem.* **15** 949

Li J T, Li M, Li J H and Sun H W 2007 *Ultrason. Sonochem.***14** 62

Lizama C, Freer J, Baeza J and Mansilla H 2002 *Catal. Today* **76** 235

Quintana M, Ricra E, Rodriguez J and Estrada W 2002 *Catal. Today* **76** 141

Savoskin M V, Yaroshenko A P, Lazareva N I, Mochalin V N and Mysyk R D 2006 *J. Phys. Chem. Solids* **67** 1205

Shornikova O N, Sorokina N E and Avdeev W 2008 *J. Phys. Chem. Solids* **69** 1168

Toyoda M and Inagaki M 2000 *Carbon* **38** 199

Tryba B, Morawski A W, Kalenczuk R J and Inagaki M 2003 *Spill Sci. Technol. Bull.* **8** 569

Wang H and Xie C S 2008 *J. Phys. Chem. Solids* **69** 2440

Yeber M C, Rodriguez J, Freer J, Baeza J, Duran N and Mansilla H 1999 *Chemosphere* **39** 1679

Yue X Q, Zhang R J, Wang W Y, Wang L Q and Yang Y L 2008 *Mater. Lett.* **62** 1919

Zheng Y P, Wang H N, Kang F Y, Wang L N and Inagaki M 2004 *Carbon* **42** 2603